ELSEVIER

Journal of Nuclear Materials 266–269 (1999) 648–653

journal of nuclear materials

Experimental investigation of the effects of neon injection in TCV

R.A. Pitts *, A. Refke, B.P. Duval, I. Furno, B. Joye, J.B. Lister, Y. Martin, J.-M. Moret, J. Rommers, H. Weisen

Centre de Recherches en Physique des Plasmas, Association EURATOM-Conféderation Suisse, École Polytechnique Fédérale de Lausanne, CH-1015 Lausanne, Switzerland

Abstract

This contribution describes the results of impurity seeding experiments using neon gas injection into the private flux zone of an ohmically heated TCV single null lower, deuterium fuelled, open divertor configuration. In these first experiments, neon has been injected under feedback control on the intensity of the UV NeVIII line at 77 nm. Measurements of the dependence of edge temperature and density on $\bar{n}_e$ at the outboard divertor target show the divertor in the absence of neon to be operating in the low recycling regime. Neon is observed to penetrate easily into the confined plasma at all densities, increasing core radiation and suppressing radiation in the divertor. This suppression is accompanied by reductions of power and particle flux to the divertor target and D_α emission in the divertor volume. The most intense emission is observed in the X-point vicinity and stable discharges have been obtained at radiation fractions, P_R/P_Ω, up to 0.75. Values of $\langle Z_{eff}\rangle = 1.5$–2 and $\langle \Delta Z_{eff}\rangle = 0.25$–0.75 are observed at the highest densities for which the lowest core neon concentrations of $\approx$0.5–1.0% are obtained, with $\langle Z_{eff}\rangle$ appearing to scale with P_R and and $\bar{n}_e$ according to the empirical relationship derived by Matthews (G.F. Matthews et al., J. Nucl. Mater. 241–243 (1997) 450). There is evidence for an increase in particle confinement when neon is injected, with the effect being most marked at the highest densities when the radiated power fractions are highest. Neon injection is also found to be effective in suppressing ohmic H-modes.

Keywords: TCV; Detached plasma; Neon injection; Single-null divertor; Radiation

1. Introduction

An earlier paper [1] described the results of recycling studies on TCV ($R = 0.89$ m, $a = 0.25$ m, $B_\phi = 1.43$ T) performed using a reference single null lower (SNL) diverted configuration particularly well suited to the edge diagnostics both presently available and planned. Density ramp experiments up to the density limit in this type of discharge with no external impurity injection have produced only partial detachment very close to the outboard strike point at the highest densities (there are presently no reliable measurements at the inner strike point). To provoke a greater degree of detachment, impurity seeding experiments have been performed using neon gas injection, primarily because the recycling nature of neon makes for easier control of injected impurities. In coronal equilibrium, the neon emissivity peaks at rather high temperatures ($T_e = 40$ eV [2]), so that radiation from neon would not be expected to be confined to the TCV divertor region in the absence of any additional heating to increase the edge temperature. The results presented here corroborate this simple expectation and, whilst divertor detachment is easily achieved when neon is injected, it is due rather to a strong reduction in the power flow reaching the edge plasma than to the processes of momentum removal and recombination seen in the divertors of larger machines characterised by strong, parallel field gradients of n_e and T_e [3].

* Corresponding author. Tel.: +44 21 693 60 03; fax: +44 21 693 51 76; e-mail: richard.pitts@epfl.ch.

0022-3115/99/$ – see front matter
PII: S0022-3115(98)00599-6

2. Experiment

The rather open geometry of the diverted discharge ($\kappa_{95} = 1.6$, $\delta_{95} = 0.35$) used in this study is shown in Fig. 1. Graphite protection tiles covered ≈65% of the vacuum vessel internal surface area and the last boronisation was performed some 800 tokamak discharges before the start of these experiments. Neon is injected from the lower inside corner of the vessel, directly into the private zone of the SNL equilibrium, with the deuterium gas fuelling (controlled by density feedback) through a lower middle port. A visible OMA spectrometer observes emission from the NeIII (Ne^{2+}) line at 259 nm and a VUV spectrometer that from the NeVIII (Ne^{7+}) line at 77 nm. For these experiments, neither the spectrometers nor the neon gas influx were absolutely calibrated so that details of the neon particle inventory are unfortunately unavailable. The neon gas flux rate is feedback controlled using the intensity of the NeVIII line such that higher plasma densities lead to lower core plasma neon concentrations, C_{Ne}, for fixed line intensity.

Outboard divertor target parameters are measured with an array of tile mounted, domed single Langmuir probes and a scanning IR TV camera viewing the vessel floor from above. An array of 5 total radiation bolometer cameras with a maximum of 64 viewing chords is used to tomographically reconstruct the 2-D radiation distribution (across the full poloidal cross-section). Soft X-ray emission is also monitored using a similar camera array with somewhat higher spatial resolution. Line integrated measurements of IR Bremsstrahlung for viewing chords passing through the plasma core [4] are combined to provide $\langle Z_{eff} \rangle$, the volume averaged effective charge, values of which can be compared with those computed from analysis of the soft X-ray emission.

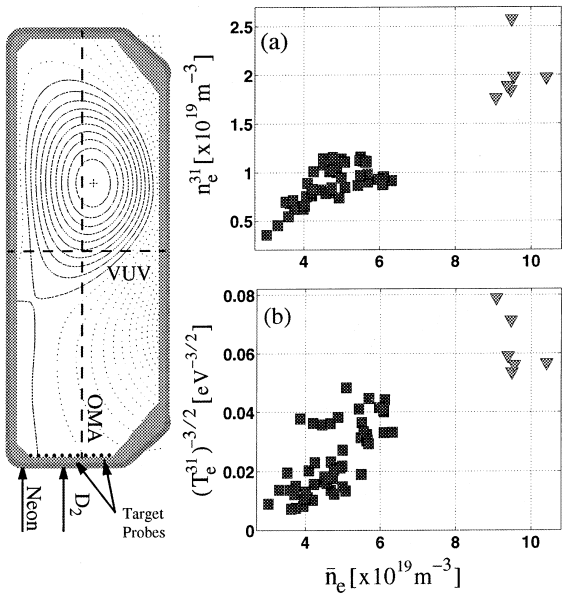

Fig. 1. (Left) The SNL configuration used for the neon injection. (Right) The dependence on $\bar{n}_e$ *in the absence of neon* of (a) n_e and (b) $T_e^{-3/2}$ for target Langmuir probe 31 located 5–6 cm from the outer strike point. (■) $I_p = 280$ kA, (▼) $I_p = 380$ kA.

Discharges have been run almost exclusively at $I_p = 280$ kA, with a few at $I_p = 380$ kA and in all cases the ∇B drift is directed away from the X-point. The curves to the right of Fig. 1 show the variation with line average central density, $\bar{n}_e$ *in the absence of neon*, of n_e and $T_e^{-3/2}$ for a probe located an average of 5–6 cm from the outboard strike point, corresponding to 4–5 mm from the separatrix at the outside midplane. At this position in the scrape-off layer (SOL), the midplane to outboard target plate connection length, $L_{con} \approx 26$ m for $I_p = 280$ kA with a flux expansion of 11. The linear dependence on density seen in both cases is what would be expected if the divertor were operating in the sheath limited, or low recycling regime [3]. For the data of Fig. 1, $L_{con}/\lambda_{ee} \approx 5$ and so the outboard SOL is only mildy collisional in these discharges.

3. Results

3.1. Time variation of a single discharge

A series of L-mode discharges at $I_p = 280$ kA have been performed in which the plasma density is varied for two values of the feedback NeVIII line intensity, with the highest value being approximately double the lowest. The two levels are chosen empirically on the basis of the effect observed on the divertor plasma (Section 3.2). Fig. 2 illustrates the time history for a discharge in the group with higher NeVIII feedback intensity. Neon first enters the discharge at $t \approx 0.55$ s, before which the tomographic reconstruction shows the radiation distribution to be localized at and below the X-point. The 2-D bolometry data are used in conjunction with the magnetic equilibrium reconstruction to separate contributions to the radiation from inside, P_R^{IN} and outside, P_R^{OUT} the separatrix (the accuracy is limited near the X-point where spatial resolution is rather poor.) These contributions are plotted in Fig. 2(c), indicating an approximate ratio of $P_R^{OUT}/P_R^{IN} \approx 2.5$ before neon injection. Note that P_R^{OUT} comprises the radiation both below the X-point and around the main plasma separatrix.

The arrival of neon in the plasma provokes a *simultaneous* decrease in radiation everywhere in the divertor (there is no smooth movement of a radiation front up to the X-point) accompanied by a decrease in D_α emission in the divertor (Fig. 2(g)) and a reduction of particle (Fig. 2(h)) and power flow (Fig. 2(i)) to the outboard target tiles. The probe power in Fig. 2(i) is computed assuming $T_i = T_e$ and a sheath heat transmission factor,

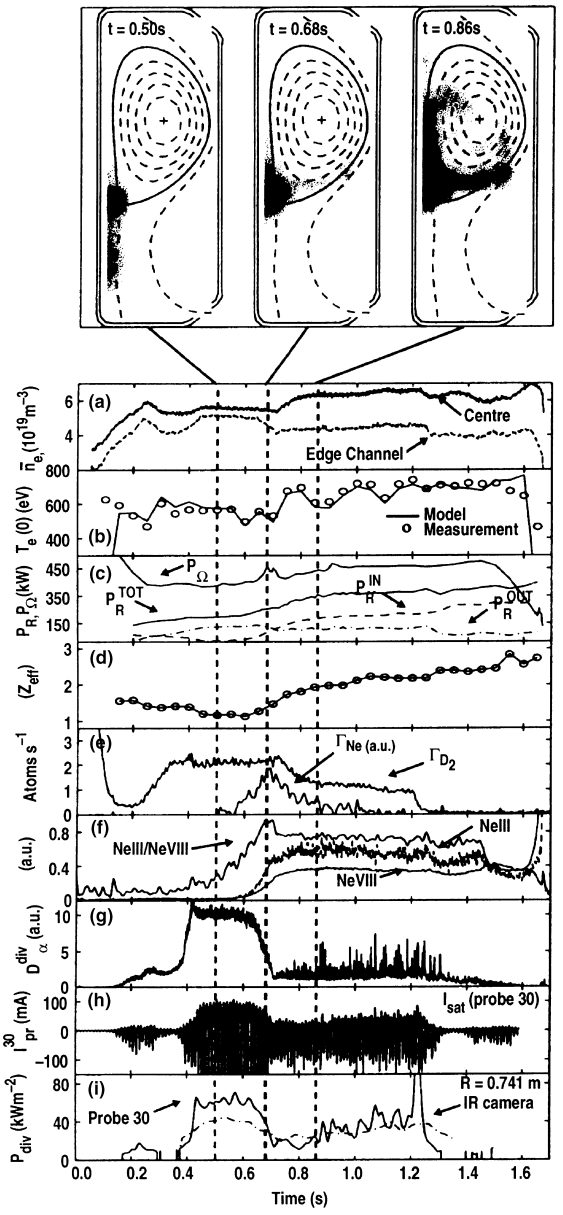

Fig. 2. Time history of relevant signals for TCV shot #13410 showing the plasma response to neon injection for a discharge with $I_p = 280$ kA. The 3 vertical dotted lines indicate the times at which the radiation distributions above the figure have been computed. Details of the meaning of each trace may be found in the text.

$\gamma = 7$. The intensities of both the NeIII and NeVIII lines increase [Fig. 2(f)], P_R^{TOT} increases and P_R^{IN} begins to increase as P_R^{OUT} decreases (Fig. 2(c)). During the rise time of the neon gas injection, the NeIII/NeVIII line ratio [Fig. 2(f)] increases, reaching a peak value at the maximum of the injected neon gas flux and thereafter remaining roughly constant as the discharge progresses, even after the feedback has closed the neon injection valve. The constancy of the line ratio indicates that no core impurity accumulation is occurring.

The time at which $P_R^{OUT} = P_R^{IN}$, corresponds to the point at which both j_{sat} and T_e have decreased by factors between 3 and 4 across the divertor floor and the edge plasma is now effectively starved of power (the spikes visible on the D_α signal in Fig. 2(g) are due to the now more pronounced effect of sawtooth heat pulses arriving in the divertor volume). The reduction in divertor density may also be seen from the behaviour of $\bar{n}_e$ measured by an interferometer chord passing vertically through both the confined plasma and the outboard divertor leg (dashed line in Fig. 2(a)), which attains the same value after neon as earlier in the discharge before the divertor is formed at $t = 0.43$ s.

Beyond the cross-over point in P_R^{OUT} and P_R^{IN} when the effect on the divertor has reached its maximum, the core plasma parameters begin to be affected, with $T_e(0)$, Z_{eff} and $\bar{n}_e$ all increasing. This indicates that in the early stages of injection at least, the divertor is partially efficient in shielding the passage of the neon atoms into the confined plasma. Quasi steady-state is attained for $t > 0.9$ s, by which time V_{loop} (not shown) has increased by 25% relative to its pre-neon value, leading to an increase in P_Ω (Fig. 2(c)). The radiation is now concentrated inside the separatix with $\langle \Delta Z_{eff} \rangle = 1$ (Fig. 2(d) – IR Bremsstrahlung measurement) and $P_R^{TOT}/P_\Omega = 0.7$ for $C_{Ne} = n_{Ne}/n_e \approx 1\%$. At $t = 1$ s, the total radiated powers inside normalized radius $\rho \approx 0.55$ computed from bolometry and X-ray emissivity (corrected for the Berylium filter transmission) are in excellent agreement for this discharge, giving $P_R \approx 50$ kW. This should be compared with $P_R^{IN} = 190$ kW and $P_R^{TOT} = 318$ kW at the same time in the discharge. Outside this central region, the poloidal radiation distribution is strongly asymmetric and is concentrated in the X-point region. Thomson scattering measurements at $\rho \approx 0.95$–0.97 show T_e and n_e there to decrease in the presence of neon.

Since the line averaged density is feedback controlled, the 15% increase in $\bar{n}_e$ following neon injection seen in Fig. 2(a) is rather surprising. In response to this increase, the D_2 gas flux falls by $\approx$40% (see also Fig. 2(e)), but the total number of electrons in the discharge remains approximately constant. In fact, for this discharge the neon injection leads to a peaking of the density profile, with the central density, $n_e(0)$, rising from 6×10^{19} m^{-3} before neon to 8.5×10^{19} m^{-3} in steady-state with neon present. This, together with the decrease in D_α emission implies an increase in particle confinement, τ_p, although quantitative estimates of the magnitude of the increase depend on more detailed knowledge of the recycling behaviour of both the deuterium and neon species than is possible with the currently available measurements. The reduced transparency of the divertor plasma during neon injection will modify the deuterium

fuelling efficiency and it is unclear how the cool edge influences the neon transport in this region. Similar profile peaking is observed in other discharges in the series, but the effect is always most marked for the highest densities with high feedback NeVIII line intensity. Such peaking of the density profile has also been observed in the TEXTOR and ASDEX Upgrade tokamaks during highly radiative discharges at high $\bar{n}_e$ [5,6] with strong additional heating. The phenomena is currently the subject of some discussion and is not completely understood.

Associated with the rise in $n_e(0)$ is an increase in electron energy confinement, τ_{Ee}, of some 25%. The combination of changes in τ_{Ee}, $n_e(0)$ and plasma resistivity lead to a change in $T_e(0)$ that scales like $T_e(0) \propto [j^2(0)\tau_{Ee}/3ec_\sigma n_e(0)]^{2/5}$ [7], where $j(0)$ is the central current density and c_σ the Spitzer conductivity coefficient depending on $Z_{eff}(\sigma_{spitzer} = c_\sigma T_e^{3/2})$. This relationship has been used to compute the expected $T_e(0)$ for the discharge in Fig. 2 and the result is included with the measured value in Fig. 2(b). Agreement is clearly excellent throughout the discharge, demonstrating that Spitzer resistivity is a good description of the response of these discharges to the impurity seeding.

3.2. Radiation and Z_{eff}

Fig. 3 illustrates the density dependence of the ratios P_R^{OUT}/P_R^{IN} and P_R^{SOL}/P_R^{DIV}, where P_R^{SOL} is the radiation emanating from outside the main plasma separatrix and P_R^{DIV} that emitted from below the X-point and taken as a crude measure of the outboard divertor radiation. Data points are obtained by averaging signals over a 40 ms time interval centred around time points selected during steady-state before and after neon injection. No attempt has been made in these discharges to investigate systematically the maximum radiation fraction that can be sustained without disruption.

Since varying the density at fixed NeVIII line intensity leads automatically to varying neon concentration, the data in Fig. 3 are grouped into three ranges of C_{Ne}. The latter is obtained from emissivities tabulated as functions of T_e assuming coronal equilibrium using the IONEQ, ionisation equilibrium and radiation code (courtesy A. Weller, IPP Garching) [8]. The local neon concentration is then inferred from the tomographically reconstructed soft X-ray emission using the tabulated emissivities for neon, carbon and deuterium and assuming that the concentration of carbon remains unchanged from that prevailing before neon injection. This calculation yields flat Z_{eff} profiles, with the central values of Z_{eff} in good agreement with those derived from line integrated measurements of IR Bremsstrahlung using the measured density and temperature profiles.

Neon is clearly effective at all densities in switching the balance of radiation in the edge, with comparatively

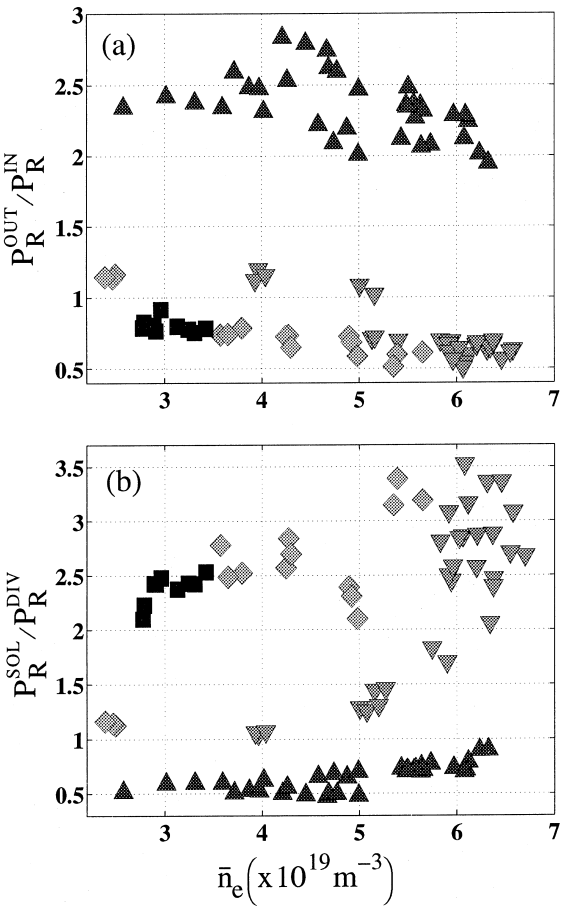

Fig. 3. Variation of the ratio P_R^{OUT}/P_R^{IN} (a) and P_R^{SOL}/P_R^{DIV} (b) with $\bar{n}_e$ for different effective neon concentrations at $I_p = 280$ kA. The approximate real concentrations (in % of the total number of electrons) derived from IR Bremsstrahlung and soft X-rays are: (▲) No neon, (▼) $0.25 < C_{Ne} \leqslant 1.2$, (♦) $1.2 < C_{Ne} \leqslant 2$, (■) $2 < C_{Ne} \leqslant 2.5$. To improve statistics, several points have been extracted from different times in each discharge but always during steady-state before and after neon injection.

smaller concentrations being required to effect the switch as density increases. The Ne^{7+} line intensity is also evidently a direct indicator of the main plasma radiation level (and has been used in other experiments for feedback on P_R^{IN} [9]), in agreement with the IONEQ simulations showing the maximum radiative power of the Ne^{7+} species to occur at $T_e \approx 50$ eV for these discharges. This corresponds to the temperature measured just inside the separatrix by Thomson scattering.

The two groups of discharges are clearly visible in Fig. 3. For the case of no neon injection and for the lowest of the two feedback line intensities, $P_R^{OUT}/P_R^{IN} \geqslant 1$. In the latter case, the effect on the divertor plasma of the neon injection is less marked, with

decreases in edge T_e and n_e of a factor of 2 maximum noted close to the separatrix but not elsewhere in the outboard divertor fan. Radiation fractions are thus lower and the SOL is less starved of power. At the higher feedback line intensity (the discharge of Fig. 2 is a good example), $P_R^{OUT}/P_R^{IN} < 1$, $P_R^{SOL}/P_R^{DIV} > 1$ and the divertor no longer contributes significantly to the total radiation balance.

In Fig. 4, the observed values of $\langle Z_{eff}\rangle$ from IR Bremsstrahlung are plotted against the scaling due to Matthews [10]:

$$Z_{eff} = 1 + 5.6\left(\frac{P_R Z^{0.19}}{S^{1.03}\bar{n}_e^{1.95}}\right)$$

with S the plasma surface area ($\approx$11 m^2 for these discharges), $Z = 10$ for neon, $\bar{n}_e$ is units of 10^{20} m^{-3} and P_R in MW. Radiation from the divertor and main plasma regions has not been separated in computing P_R since the contribution from the inner divertor (with short connection lengths to the wall in the poloidal plane) is difficult to extract reliably given the poor spatial resolution of the bolometry array in this region. The data cover a broad range of $\langle Z_{eff}\rangle$, with the largest values corresponding to the lowest densities where C_{Ne} is highest and for which $\langle \Delta Z_{eff}\rangle \approx 2.5$. They have been crudely separated according to the ratio of edge to main plasma radiation distribution (Fig. 3(a)). Agreement is generally good in all cases, but, for this limited database at least, appears to be somewhat better for those discharges at lower feedback NeVIII line intensity with more equal distribution of radiation inside and outside the separatrix and hence less marked effect on the power conducted to the divertor targets.

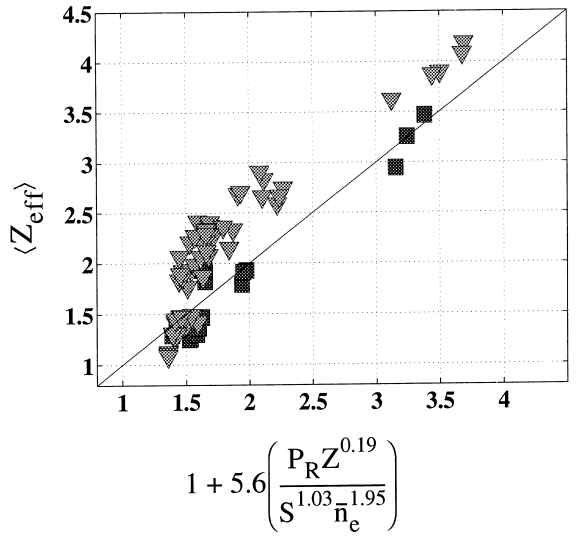

Fig. 4. Comparison of the measured volume averaged Z_{eff} with the scaling due to Matthews [10] for shots with neon injection ($Z = 10$ assumed). The data are separated according to the main/edge plasma radiation distribution and include discharges at $I_p = 280$ kA and 380 kA. (■) $P_R^{OUT}/P_R^{IN} > 1$; (▼) $P_R^{OUT}/P_R^{IN} < 1$.

3.3. Neon and ohmic H-mode

Despite the unfavourable ∇B drift direction, ohmic H-mode transitions have been observed in some of the discharges at $I_p = 380$ kA into which neon was injected. The traces in Fig. 5 summarize one such example in which neon first enters the plasma at 0.55 s, reaching a

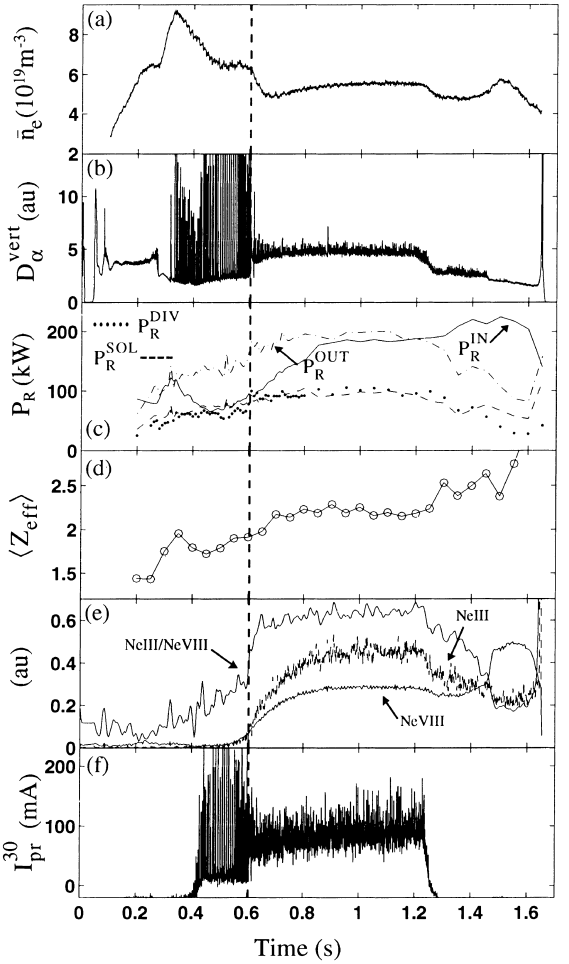

Fig. 5. TCV discharge #13459 with $I_p = 380$ kA in which an ohmic H-mode (L–H transition at $t = 0.273$ s) is terminated by neon injection beginning at $t = 0.55$ s. The time of the H–L transition is indicated by the vertical dashed line. (a) $\bar{n}_e$ along the central chord, (b) D_α for a chord passing vertically through the machine center, (c) separated components of radiation distribution, (d) volume averaged Z_{eff}, (e) NeIII, NeVIII line intensities and their ratio, (f) I_{sat} to a target probe located 2–3 cm from the outboard strike point.

final concentration of ≈0.5% in the plateau phase. The H-mode transition occurs at 0.27 s, when the X-point is first formed, followed by a short ELM-free period and then a burst of ELMs before the H–L transition at 0.6 s (see the D_α trace in Fig. 5(b)). The radiation fractions in Fig. 5(c) illustrate how $P_R^{DIV} = P_R^{SOL}$ throughout the discharge and how $P_R^{OUT} = P_R^{SOL} + P_R^{DIV} \approx 2P_R^{IN}$ during the ELMing phase before neon is injected. Later, with neon present, $P_R^{OUT} \approx P_R^{IN}$ and the impurity concentration is insufficient to produce complete detachment at the edge. This can also be seen in the Langmuir probe current to probe 30, located ≈2 cm from the strike point, which remains at a high level following the H–L transition (Fig. 5(f)).

The ELMs are effective in reducing the initial density rise during the ELM-free period, establishing an equilibrium density of $\bar{n}_e = 6.5 \times 10^{19}$ m^{-3} before neon injection (Fig. 5(a)). As in the example discharge of Fig. 2, both the NeVIII and NeIII line intensities (Fig. 5(e)) increase simultaneously when the neon is injected. On this occasion, however, there is a rapid increase in the ratio NeIII/NeVIII coincident with the H–L transition, presumably reflecting changes in the edge temperature profile due to the change in confinement. Following the transition, the radiation inside the separatrix climbs steeply, despite the density decrease due to the transition to L-mode, leading to $\langle \Delta Z_{eff} \rangle \approx 0.25$ with respect to the value at the transition. It would thus appear that relatively low quantities of injected neon suffice to extinguish these ohmic H-modes, probably because the power crossing the separatrix is no longer sufficient to sustain the high confinement mode.

4. Conclusions

Impurity seeding experiments have been performed in TCV using neon injection under feedback control on the intensity of the NeVIII UV line at 77 nm. The chosen reference discharge is a single null lower diverted configuration with $I_p = 280$ kA and for which the outboard divertor plasma (where measurements have been made) is in the low recycling regime at all densities studied. Neon injection provokes rapid modifications to the plasma radiation distribution, making its way unhindered into the confined plasma at all densities and leading to a stable highly radiating zone in the vicinity of the X-point. At sufficiently high radiation fractions, the scrape-off layer becomes starved of power, leading to a loss of power and particles at the divertor target plates and radiation in the divertor volume. In these cases, peaking of the plasma density profile is observed, implying an increase in particle confinement although further work is required to quantify the changes in recycling resulting from the strong effect of neon on the divertor plasma. The measured values of Z_{eff} for these discharges are generally in agreement with the scaling of Matthews [10] with indications that agreement is best for cases in which the radiated power fractions are lower and the effect on the edge plasma less marked. For those discharges containing a transition to ohmic H-mode, neon injection appears to be efficient in provoking an H–L transition, presumably due to a reduction in the power crossing the separatrix.

Acknowledgements

The authors would like to thank the TCV team for the technical support that made these measurements possible. This work was partly supported by the Fonds National Suisse de la Recherche Scientifique.

References

[1] R.A. Pitts et al., J. Nucl. Mater. 241–243 (1997) 867.
[2] U. Samm et al., Plasma Phys. Control Fusion 35 (1993) B167.
[3] C.S. Pitcher, P.C. Stangeby, Plasma Phys. Control Fusion 39 (1997) 779.
[4] J.H. Rommers et al., 8th Int. Symposium on Laser Aided Plasma Diagnostics, Doorwerth, The Netherlands, 22–26 September 1997.
[5] A. Messian et al., Nucl. Fusion 34 (1994) 825.
[6] A. Kallenbach et al., Plasma Phys. and Control Fusion 38 (1996) B167.
[7] H. Weisen et al., Nucl. Fusion 37 (1997) 1741.
[8] H. Weisen et al., Rev. Sci. Instrum. 62 (1991) 1531.
[9] G.L. Jackson et al., J. Nucl. Mater. 241–243 (1997) 618.
[10] G.F. Matthews et al., J. Nucl. Mater. 241–243 (1997) 450.